Valley splitting in strained silicon quantum wells

Timothy B. Boykin
Department of Electrical and Computer Engineering, University of Alabama in Huntsville, Huntsville, Alabama 35899

Gerhard Klimeck
Jet Propulsion Laboratory, California Institute of Technology, Pasadena, California 91109

M. A. Eriksson, Mark Friesen, and S. N. Coppersmith
Department of Physics, University of Wisconsin, Madison, Wisconsin 53706

Paul von Allmen, Fabiano Oyafuso, and Seungwon Lee
Jet Propulsion Laboratory, California Institute of Technology, Pasadena, California 91109

(Received 15 August 2003; accepted 10 November 2003)

A theory based on localized-orbital approaches is developed to describe the valley splitting observed in silicon quantum wells. The theory is appropriate in the limit of low electron density and relevant for quantum computing architectures. The valley splitting is computed for realistic devices using the quantitative nanoelectronic modeling tool NEMO. A simple, analytically solvable tight-binding model reproduces the behavior of the splitting in the NEMO results and yields much physical insight. The splitting is in general nonzero even in the absence of electric field in contrast to previous works. The splitting in a square well oscillates as a function of S, the number of layers in the quantum well, with a period that is determined by the location of the valley minimum in the Brillouin zone. The envelope of the splitting decays as S^{-3}. The feasibility of observing such oscillations experimentally in Si/SiGe heterostructures is discussed. © *2004 American Institute of Physics.* [DOI: 10.1063/1.1637718]

There is much interest in developing semiconducting nanostructures in which spins are coherent: for example a spin-based quantum dot quantum computer.[1] Reasons for using silicon as opposed to gallium arsenide heterostructures include (1) longer intrinsic spin coherence times due to smaller spin-orbit coupling and (2) elimination[2] of decoherence caused by coupling between electrons and nuclear spins by use of isotropically pure spin-zero ^{28}Si. However, one complication of Si compared to GaAs is that unstrained Si has a sixfold degenerate conduction-band minimum. Strain in Si/SiGe heterostructures reduces the sixfold valley degeneracy to be twofold, but the remaining twofold valley degeneracy is a potential source of decoherence and other difficulties.[3] It is thus of great interest to understand how to lift this remaining two-valley degeneracy and maximize the energy splitting between the lowest quantized levels.

Valley splitting has been studied experimentally[4] and theoretically.[5] Early work includes the effective mass approaches of Sham and Nakayama[6] at single interfaces, and Ohkawa[7] in quantum wells. More recently, Grosso[8] used an sp^3 empirical tight-binding model to study the splitting in Si superlattices. None of these works focus on the essential differences in the behavior of the valley splitting in triangular versus square wells. However, modern heterostructures have now made square well potentials much more experimentally relevant. Ohkawa[7] has found the essential features of the valley splitting in finite quantum square wells: the presence of a nonzero splitting even in zero electric field; the oscillation of the splitting as a function of quantum well thickness; and the decay of the splitting as the cube of the well thickness. However, Ohkawa did not appreciate the essential role of the square well potential in obtaining these results. Moreover, Ohkawa's methods have been criticized;[5] an important conceptual problem is that his multiband effective mass theory uses a k-state basis, fundamentally inappropriate for a quantum-confined structure, and includes a structure-specific intervalley-coupling constant.

Here the empirical tight-binding method is used to study valley splitting in the limit of low electron density. The localized-orbital basis used in tight binding is most appropriate for heterostructures, which have large changes of the potential on the atomic length scale.

Figure 1(a) shows the valley splitting versus well width at various electric fields for strained Si [001] quantum wells with hard wall boundary conditions using strain conditions appropriate for a $Si_{0.8}Ge_{0.2}$ relaxed substrate. The results were obtained using the Nanoelectronic Modeling tool,

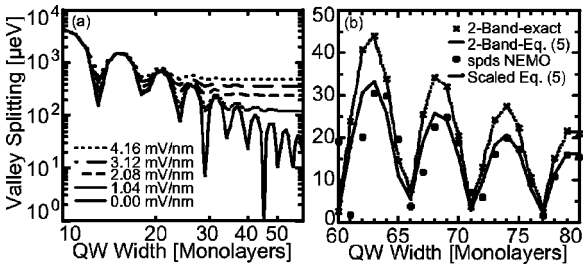

FIG. 1. Valley splitting vs well width in a strained Si quantum well. (a) splitting at various applied E fields using NEMO's $sp^3d^5s^*$ model, with integral numbers of monolayers; (b) comparison of NEMO results at zero applied field vs simple tight binding model. Symbols show NEMO (●) and two-band (×) results evaluated at atom sites. Lines (with interpolation) are Eq. (5), as written (dotted), or scaled to better match NEMO (dashed); scaling is justified by the many evanescent states absent from the simpler models.

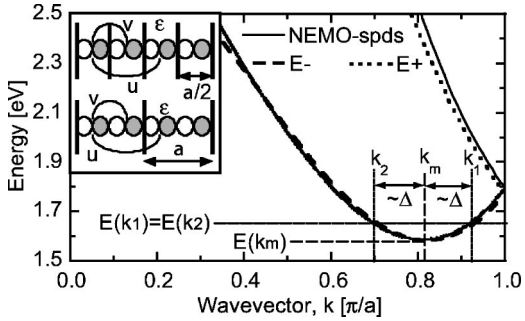

FIG. 2. Bulk dispersion from NEMO and Eq. (1). Valley splitting arises when there are two pairs $(k_{1,2},-k_{1,2})$ of counterpropagating bulk states forming two degenerate bound states with the proper cosine-like envelope at a given energy. Under confinement to length L this envelope is characterized by $(k_1-k_2)/2\approx\Delta\approx\pi/L$ for energy $E(k_1)=E(k_2)$. In the parlance of perturbation theory, confinement couples these two degenerate states, when splitting of the lowest two QW eigenstates, each of which is characterized by a pair of bulk states $(k_1^{e,o},k_2^{e,o})$ for even and odd parity. Roughly, the envelopes of both lowest eigenstates are this same cosine, while the rapid oscillations determined by $(k_1+k_2)/2\approx k_m$ are of opposite parity [Fig. 3(a)]. Inset: Sketch of two versions of a simple *p*-orbital tight-binding model, related by a basis change; positive lobes are shaded, negative white. Upper: Single-band model with one *p*-like orbital per atom and one atom per unit cell (size $a/2$). Parameters are ϵ (onsite), v (nearest-neighbor), and u (second-near-neighbor). Lower: Doubling the unit cell to two atoms (size a) yields a two-band model.

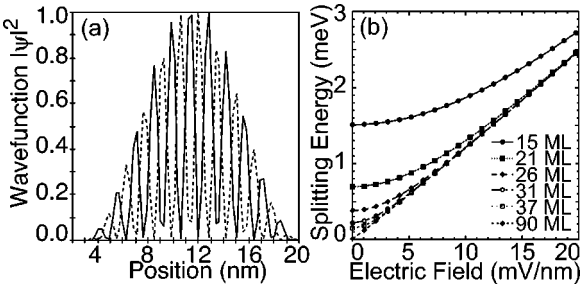

FIG. 3. (a) Typical NEMO wave functions (trace over tight binding coefficients) of two valley-split states; (b) valley splitting in a strained Si quantum well with hardwall boundary conditions versus applied field for several well widths in monolayers, calculated NEMO.

NEMO,[9] a heterostructure modeling tool that simulates high bias transport across heterostructure layers using the nonequilibrium Green function formalism. NEMO has been used[9] for the quantitative design of resonant tunneling diodes, MOS oxide thickness analysis and studies of incoherent scattering. Here a nearest-neighbor, tight-binding, spin-orbit $sp^3d^5s^*$ model[10] with 40 orbitals per unit cell, recently updated for strained SiGe systems is used. NEMO provides a highly accurate picture of the atomic-scale structure of electronic wave functions in a silicon quantum well in the limit of low electron densities appropriate for quantum computing. Three features of the calculation stand out: (i) the splitting is nonzero even at zero field; (ii) the zero field splitting exhibits oscillations as a function of well width; and (iii) the envelope decays as the cube of the well thickness.

While NEMO gives results of high accuracy, the sheer number of bands in the model blur the underlying (simple) physics. Two simple models that are related through basis transformations (Fig. 2) are developed to gain more insight; only the two band is considered here.[11]

The bulk (cyclic boundary) version of the tight-binding model has the dispersion relations

$$E_{\pm}(k)=\epsilon\pm 2v\cos(ka/2)+2u\cos(ka), \tag{1}$$

where $a=2.715$ Å is the length of a unit cell. Fitting Eq. (1) to bulk dispersion curves obtained from NEMO (Fig. 2), to obtain the same degenerate valley minima and curvature, yields $v=0.683$ eV and $u=0.612$ eV.

The energy difference E_{21} between the two low-lying eigenstates in the finite two-band model is now calculated without additional fitting parameters, as shown in Fig. 1(b). Since NEMO incorporates spin-orbit coupling while the two-band model does not, it is clear that spin-orbit coupling is irrelevant.[12] The excellent agreement with the sophisticated NEMO calculation in terms of the oscillations and their envelope shows that the two-band model captures the essential physics of valley splitting.

To obtain analytic expressions for the valley splitting of the model of Fig. 2, we write the wave function in the localized-orbital basis for a chain of $2N+1$ unit cells (each unit cell of the chain represents a monolayer in [001]-oriented Si) centered at the origin, as

$$|\psi\rangle=\sum_{j=-N}^{N}[C_j^{(\alpha)}|\alpha;ja\rangle+C_j^{(\beta)}|\beta;ja\rangle], \tag{2}$$

where α and β are the localized orbitals. Each energy of interest for valley splitting lies in the valley of the lower band with two Bloch states k_1 and k_2, satisfying Eq. (1):

$$E_-(k_1)=E_-(k_2). \tag{3}$$

At each energy, the localized-orbital expansion coefficients, C, can be expressed in terms of these two bulk states.[13] Due to inversion symmetry the eigenstates of Eq. (2) are simultaneous parity eigenstates. The even states are linear combinations of cosines at k_1 and k_2, while the odd states are linear combinations of sines. The hard wall condition implies

$$C_{N+1}^{(\alpha)}=C_{N+1}^{(\beta)}=0,\quad C_{-(N+1)}^{(\alpha)}=C_{-(N+1)}^{(\beta)}=0. \tag{4}$$

The very different physics of quantum-confined states in direct- and indirect-gap quantum wells is a consequence of the bulk bands together with Eqs. (2)–(4). In both cases degenerate Bloch states $\pm k$ may be combined so that the coefficients are sines and cosines. In a direct-gap well there is only one pair of Bloch states at each energy, so that (evanescent states aside) the hardwall condition can only be satisfied by doubling k on going from the ground to the first excited state. In contrast, for an indirect gap well, the hardwall condition may be satisfied by not only altering the values k_1 and k_2, but also their mixture. Hence the lowest two states are characterized by pairs (k_1^e,k_2^e), (k_1^o,k_2^o) differing slightly, so that the lowest even and odd states have cosine-like envelopes with $(k_1^{e,o}-k_2^{e,o})/2\approx\pi/L$ [Fig. 3(a)].

For a quantum well of S atoms $[S=2(2N+1)]$, Eqs. (3) and (4) can be solved analytically[11] order-by-order in powers of $(S+2)^{-1}$. To leading order in $(S+2)^{-1}$, the splitting, denoted E_{21}, is

$$E_{21}\simeq\frac{16\pi^2u}{(S+2)^3}|\sin[(S+2)\phi_0]|\sin(\phi_0), \tag{5}$$

where $\phi_0 = k_m a/2$ and $\sin(\phi_0) = \sqrt{1-(v/4u)^2}$. Higher-order corrections to Eq. (5) can be calculated in a straightforward manner;[11] these corrections are modest down to quantum well widths of order 40 unit cells.

Equation (5) predicts a decay in the amplitude of the oscillations with $(S+2)^{-3}$. The oscillations with well width have a frequency determined by the location of the valley minimum k_m, and are a direct consequence of the phase matching at the interface becoming almost identical for the two lowest states. A corollary of this oscillatory behavior is that the parity of the ground state alternates between even and odd. The alternating parity has already been noted,[14] but has not been explained.

All considerations described above are based on the assumption of a flat band quantum well. However, local electric fields are ubiquitous in heterostructures due to modulation doping and external gate potentials. Figure 1(a), which displays the splitting versus well width for different values of constant electric field, demonstrates that the field has little effect until the voltage drop per unit cell is of the same order as the splitting at zero field. For a fixed field the oscillations are quenched for longer wells; this result is reasonable since in longer wells the states are more readily localized in the bottom of the triangular notch, where they are insensitive to the location of the far boundary. Figure 3(b) shows the splitting versus applied field for quantum wells of various length calculated with NEMO. The splitting for a fixed well size increases monotonically as a function of field, becoming linear for higher fields, in agreement with Sham and Nakayama's result for semi-infinite systems.[6] However, at lower fields the splitting in a quantum well is markedly nonlinear, in contrast to the semi-infinite system.[6]

All discussions above consider infinite hard wall confinement. The effect of a finite voltage discontinuity at the well edges have also been investigated using NEMO and the two-band model. The behavior is qualitatively unaffected down to band offsets of a few tenths of an eV, so the results obtained for infinite square wells should also be realistic guide to actual heterostructures.[15]

Finally we relate the results here to experimental measurements of valley splitting in Si quantum wells. Several groups have measured nonzero valley splittings with magnitude of the same order as predicted by our models;[4] in the past, these splittings have been usually interpreted as resulting from nonzero electric fields that are typical in modulation-doped heterostructures.[6,7] Indeed, the electric fields from the dopants at typical electron densities ($10^{11}/\mathrm{cm}^2$) are such that the voltage drop per unit cell is the same order of magnitudes as the observed splittings, which in turn are of the same order as the zero-field splitting calculated here at well widths of about 10 nm. Lowering the electron density by an order of magnitude will reduce the electric field and suppress many-body effects. The simulations and the model presented here predict that experiments on heterostructures with lower electron density will provide unambiguous evidence for the mechanism for zero-field valley splitting investigated here.

In conclusion, tight-binding calculations, explaining the valley splitting in Si quantum-confined heterostructures are presented. NEMO multiband calculations[9] give the quantitative details while two-band calculations elucidate the physics of these structures. In particular, zero-field splitting oscillations with well width are predicted and explained, reasons for the amplitude decay of the oscillation and reasons for the alternating parity of the ground state are given. Experiments to probe the oscillations in the splitting will require samples with well widths accurate to one monolayer. The results lead to a better understanding of these nanostructures.

The authors acknowledge useful conversations with R. Joynt. Work at JPL, UAH, and UW was sponsored in major proportion by the U.S. Army Research Office through the ARDA Program and directly through ARDA. The work at UW was also supported by the National Science Foundation through the MRSEC and QuBIC programs. Part of the work described in this letter was carried out at the Jet Propulsion Laboratory, California Institute of Technology under a contract with the National Aeronautics and Space Administration. Funding was provided at JPL under Grant Nos. from ARDA, ONR, and JPL.

[1] D. Loss and D. P. DiVincenzo, Phys. Rev. A **57**, 120 (1998); M. Friesen, P. Rugheimer, D. E. Savage, M. G. Lagally, D. W. van der Weide, R. Joynt, and M. A. Eriksson, Phys. Rev. B **67**, 121301 (2003).
[2] A. M. Tyryshkin, S. A. Lyon, A. V. Astashkin, and A. M. Raitsimring, preprint cond-mat/0303006.
[3] B. Koiller, X. D. Hu, and S. Das Sarma, Phys. Rev. Lett. **88**, 027903 (2002).
[4] See, e.g., A. B. Fowler, F. F. Fang, W. E. Howard, and P. J. Stiles, Phys. Rev. Lett. **16**, 901 (1966); F. F. Fang and P. J. Stiles, Phys. Rev. **174**, 823 (1968); H. Koehler, M. Roos, and G. Landwehr, Solid State Commun. **27**, 955 (1978); R. J. Nicholas, K. von Klitzing, and T. Englert, Solid State Commun. **34**, 51 (1980); J. Wakabayashi, S. Kimura, Y. Koike, and S. Kawaji, Surf. Sci. **170**, 359 (1986); V. M. Pudalov, A. Punnoose, G. Brunthaler, A. Prinz, and G. Bauer, cond-mat/0104347; R. B. Dunford, R. Newbury, F. F. Fang, R. G. Clark, R. P. Starrett, J. O. Chu, K. E. Ismail, and B. S. Meyerson, Solid State Commun. **96**, 57 (1995); S. J. Koester, K. Ismail, and J. O. Chu, Semicond. Sci. Technol. **12**, 348 (1996); P. Weitz, R. J. Haug, K. von Klitzing, and F. Schäffler, Surf. Sci. **361/362**, 542 (1996); D. Monroe, Y. H. Xie, E. A. Fitzgerald, and P. J. Silverman, Phys. Rev. B **46**, 7935 (1992); S. F. Nelson, K. Ismail, J. J. Nocera, F. F. Fang, E. E. Mendez, J. O. Chu, and B. S. Meyerson, Appl. Phys. Lett. **61**, 64 (1992); G. Stöger, G. Brunthaler, G. Bauer, K. Ismail, B. S. Meyerson, J. Lutz, and F. Kuchar, Phys. Rev. B **49**, 10417 (1994).
[5] T. Ando, A. B. Fowler, and F. Stern, Rev. Mod. Phys. **54**, 437 (1982).
[6] L. J. Sham and M. Nakayama, Phys. Rev. B **20**, 734 (1979).
[7] F. J. Ohkawa, Solid State Commun. **26**, 69 (1978).
[8] G. Grosso, G. P. Parravicini, and C. Piermarocchi, Phys. Rev. B **54**, 16393 (1997).
[9] G. Klimeck, T. B. Boykin, R. C. Bowen, R. Lake, D. Blanks, T. Moise, Y. C. Kao, and W. R. Frensley, proceedings of IEEE DRC, p. 92 (1997); R. C. Bowen, G. Klimeck, R. Lake, W. R. Frensley, and T. Moise, J. Appl. Phys. **81**, 3207 (1997); R. Lake, G. Klimeck, R. C. Bowen, and D. Jovanovic, J. Appl. Phys. **81**, 7845 (1997). Further NEMO details at http://hpc.jpl.nasa.gov/PEP/gekco/nemo.
[10] J. M. Jancu, R. Scholz, F. Beltram, and F. Bassani, Phys. Rev. B **57**, 6493 (1998).
[11] T. B. Boykin, G. Klimeck, S. N. Coppersmith, M. Friesen, P. von Allmen, F. Oyafuso, and S. Lee (unpublished).
[12] R. Kümmel, Z. Phys. B **22**, 223 (1975).
[13] In larger tight-binding models one must in general express the C in terms of all Bloch and evanescent states available at the given energy.
[14] J.-C. Chiang, Jpn. J. Appl. Phys., Part 2 **33**, L294 (1994).
[15] F. Schäffler, Semicond. Sci. Technol. **12**, 1515 (1997).